

Creating images by adding masses to gravitational point lenses

Olivier Sète, Robert Luce, Jörg Liesen*

July 20, 2018

Abstract

A well-studied maximal gravitational point lens construction of S. H. Rhie produces $5n$ images of a light source using $n + 1$ deflector masses. The construction arises from a circular, symmetric deflector configuration on n masses (producing only $3n + 1$ images) by adding a tiny mass in the center of the other mass positions (and reducing all the other masses a little bit).

In a recent paper we studied this “image creating effect” from a purely mathematical point of view (Sète, Luce & Liesen, *Comput. Methods Funct. Theory* 15(1):9-35, 2015). Here we discuss a few consequences of our findings for gravitational microlensing models. We present a complete characterization of the effect of adding small masses to these point lens models, with respect to the number of images. In particular, we give several examples of maximal lensing models that are different from Rhie’s construction and that do not share its highly symmetric appearance. We give generally applicable conditions that allow the construction of maximal point lenses on $n + 1$ masses from maximal lenses on n masses.

1 Introduction

We consider the phenomenon of multiple lensed images in the framework of gravitational microlensing. Specifically, given $n \geq 2$ point masses $m_j > 0$ at positions $z_j \in \mathbb{C}$ in the complexified lens plane, we consider the lensing map $\eta : L \rightarrow S$ from the lens plane $L = \mathbb{C} \setminus \{z_1, \dots, z_n\}$ to the light source plane $S = \mathbb{C}$,

$$\eta(z) = z - \gamma \bar{z} - \sum_{j=1}^n \frac{m_j}{\bar{z} - \bar{z}_j}, \quad (1)$$

where $\gamma \in \mathbb{C}$ is the (constant) external shear. This lens model can be seen as a generalization of the Chang-RRefsdal lens to n point masses; see [1]. Given

*TU Berlin, Institute of Mathematics, MA 4-5, Straße des 17. Juni 136, 10623 Berlin, Germany (`{sete,luce,liesen}@math.tu-berlin.de`)

a light source position (projected on the lens plane) $\zeta \in \mathbb{C}$, the (projected) images of the light source are exactly the solutions of the equation $\eta(z) = \zeta$. See [15] for a general introduction to gravitational lensing and [14] for gravitational lensing in terms of complex variables; see also [11, 6].

The important question of the maximal number of images that can be produced by a gravitational lens on n point masses modeled by (1) was answered in 2006 by Khavinson & Neumann [5]. Their result is as follows.

Theorem 1.1. *The maximal number of images that can be produced by the lensing map η in (1) is $5n - 5$ if $\gamma = 0$ and $5n$ if $\gamma \neq 0$.*

In the case of *nonzero* shear, the bound of $5n$ images can be improved slightly. As shown by An & Evans [1], the maximal number of images in that case is $5n - 1$. The “missing image” accounts for a solution to the lens equation at the point infinity in the extended complex plane; see also [7].

A particular class of point lenses that realizes the maximal number of images has been devised by Rhie [12]. Her construction (and the variant discussed in [2, 3]) has been recently studied in great detail [8]. We will very briefly recall the construction with a small *additive* mass (in contrast to her original construction in [12]).

Consider the lens on n equal point masses $m_j = 1/n$ located at the vertices of a regular polygon of a certain radius r , i.e., $z_j = re^{i\frac{2j\pi}{n}}$, and without external shear ($\gamma = 0$). This yields the lensing map

$$\eta(z) = z - \frac{\bar{z}^{n-1}}{\bar{z}^n - r^n}. \quad (2)$$

For a light source located at the origin of the lens plane, i.e., $\zeta = 0$, it is known that this lens produces $3n + 1$ images [9]. In order to arrive at a maximal lens, a tiny mass ε is added at the image position $z = 0$, i.e., we define

$$\eta_\varepsilon(z) = \eta(z) - \frac{\varepsilon}{z}. \quad (3)$$

If $\varepsilon > 0$ is sufficiently small, this “perturbation” of the lens induces $2n$ “new” images on two circles around the origin [8] (and the previous image at $z = 0$ vanishes). So the lens on $n + 1$ point masses modeled by η_ε produces $5n$ images, and thus is a maximal lens.

We recently showed (in a purely mathematical context) that this “image creating effect” of adding masses is *not specific* to the particular (symmetric) lens described by (2) [13]. Our goal here is to present some implications of the mathematical results in [13] for gravitational point lens models.

In Section 2 we present a general classification of the image creating effect that is induced by adding tiny masses to an existing lens. The results are applicable to point lens models with or without external shear. The extremal case of *maximal lensing* is studied in Section 3. To our knowledge, the only known maximal point lens models are based on the lens (2) from above. We will present conditions that allow the construction of maximal point lenses different from these lenses. We give several examples for maximal lenses.

2 Adding tiny masses to a lens

Recall that the solutions to the lens equation $\eta(z) = \zeta$ can be classified using the sign of the determinant of the Jacobian of η (e.g. [10]). In terms of Wirtinger derivatives, we find for the functional determinant of the lensing map

$$\det D\eta(z) = |\partial_z \eta(z)|^2 - |\partial_{\bar{z}} \eta(z)|^2 = 1 - |R'(z)|^2,$$

where we have abbreviated $R(z) = \bar{\gamma}z + \sum_{j=1}^n \frac{m_j}{z-z_j}$, so that $\eta(z) = z - \overline{R(z)}$.

We will call an image $z^* \in \mathbb{C}$, i.e., a solution to the equation $\eta(z) = \zeta$, a *sense-preserving* image if $|R'(z^*)| < 1$, and a *sense-reversing* image if $|R'(z^*)| > 1$. The sense-reversing images correspond to saddle images (i.e., the Jacobian of η is indefinite), whereas sense-preserving images correspond to minimum or maximum images (where the Jacobian is definite). Recall that an image is called a minimal, saddle or maximal image if it is a (local) minimum, saddle point or (local) maximum of the time delay function (induced from the lens potential corresponding to η); see e.g. [10, 11]. The characterization via $|R'|$ then follows from the equality of the Jacobian determinant of the lensing map and the determinant of the Hessian of the time delay function.

Note that the functional determinant vanishes at an image z^* only if ζ lies on a caustic (i.e., infinite magnification), and we will assume in the following that this is not the case. Further we will assume in the following that $|\gamma| \neq 1$.

We will now rephrase Theorems 3.1 and 3.14 of [13] into the setting of gravitational microlensing. In short, the following theorem can be summarized as follows: If a sufficiently small mass is inserted at position z_{n+1} of the lens plane, there will always appear some “new” images nearby z_{n+1} , and all the previously existing images will only alter their positions slightly (except for possibly z_{n+1} , if it is an image position itself). The number of new images depends on certain properties of the lensing map at z_{n+1} , which we can fully classify.

Theorem 2.1. *Let $\eta_n(z) = z - \gamma\bar{z} - \sum_{j=1}^n \frac{m_j}{\bar{z}-\bar{z}_j} = z - \overline{R(z)}$ be the lensing map corresponding to $n \geq 2$ point masses $m_j > 0$ at positions $z_j \in \mathbb{C}$ with external shear $|\gamma| \neq 1$. Denote by $m_{n+1} > 0$ a tiny mass and $z_{n+1} \in \mathbb{C}$, $z_{n+1} \neq z_j$ for $1 \leq j \leq n$, a point on the lens plane at which the mass is added, i.e., consider the lensing map*

$$\eta_{n+1}(z) = \eta_n(z) - \frac{m_{n+1}}{\bar{z}-\bar{z}_{n+1}}.$$

If m_{n+1} is sufficiently small, and if the source ζ does not lie on a caustic of η_n or η_{n+1} , then there exists an open disk D around z_{n+1} such that $D \setminus \{z_{n+1}\}$ contains no mass point of η_n and no image of ζ under η_n . Further η_n and η_{n+1} have the same number of images outside D , and the following holds:

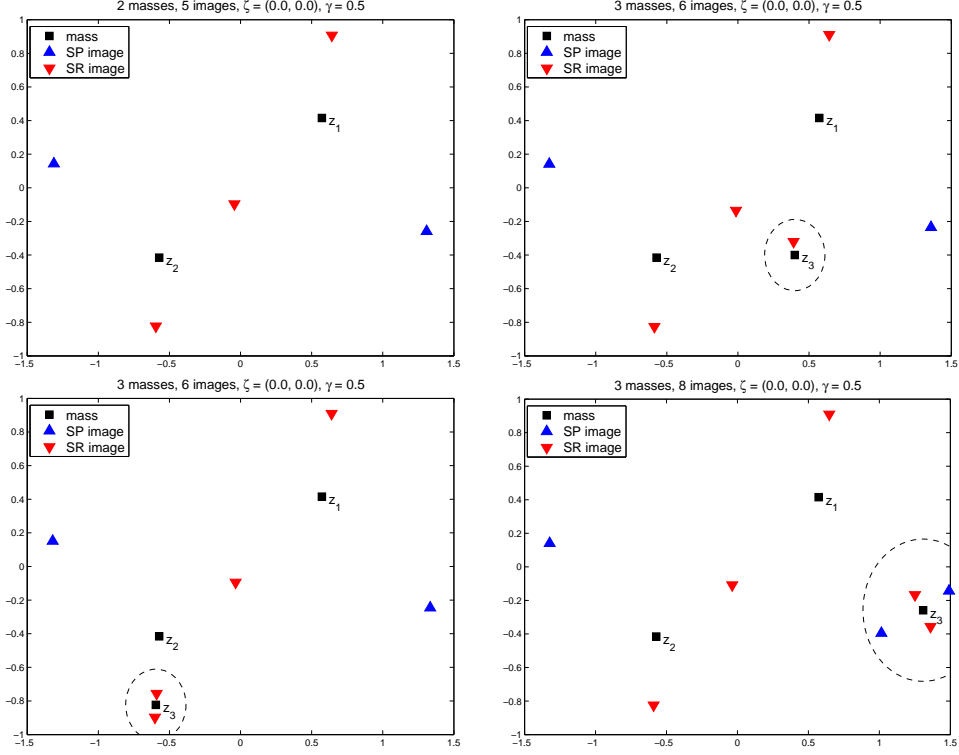


Figure 1: Illustration for Theorem 2.1. The black squares indicate mass points, and triangles show the location of the induced images of the light source. The images are classified by “SP” (sense-preserving, blue, upward pointing) and “SR” (sense-reversing, red, downward pointing). The initial binary lens is shown in the top left picture. The other pictures show the lens after adding a mass at the indicated point z_3 , which is no image (top right), a sense-reversing image (bottom left) and a sense-preserving image (bottom right) of the initial lens.

1. If z_{n+1} is not an image of ζ under η_n , then η_{n+1} has at least one image of ζ in D .
2. If z_{n+1} is a sense-reversing image of ζ under η_n , then η_{n+1} has at least two images of ζ in D .
3. If z_{n+1} is a sense-preserving image of ζ under η_n , and $|R'(z_{n+1})| \neq 0$, then η_{n+1} has at least four images of ζ in D .
4. If z_{n+1} is a sense-preserving image of ζ under η_n , $R'(z_{n+1}) = \dots = R^{(d-2)}(z_{n+1}) = 0$, and $R^{(d-1)}(z_{n+1}) \neq 0$, then η_{n+1} has at least $2d$ images of ζ in D .

Remark 2.2. 1. The lens (3) in the introduction is covered by case 4 in the preceding theorem with $m_{n+1} = \varepsilon$ and $d = n$. For this lens, appropriate values of m_{n+1} are completely characterized in [8].

2. In cases 2–4, the point z_{n+1} is –of course– no longer a solution of the lens equation $\eta_{n+1}(z) = \zeta$.
3. The lenses modeled by η_n and η_{n+1} have the same number of images outside D , and these images are located at approximately the same positions and retain their type (sense-reversing or sense-preserving).
4. If one and two images are created in cases 1 and 2, respectively, these images are sense-reversing. In cases 3 and 4 an equal number of sense-reversing and sense-preserving images are created; see [13, thms. 3.1, 3.14].
5. In all cases of the above theorem, it is guaranteed that “at least” a certain number of images are created (provided that m_{n+1} is sufficiently small). We believe that in fact no more than the stated number of images are created, and extensive numerical experiments support this claim. A mathematical proof of this claim is, however, a topic of future research.
6. The effect of adding a mass larger than the “sufficiently small” mass in the previous theorem is twofold: Either the mass is so large that the lens is globally affected and images of η_n “far away” from z_{n+1} may disappear. Otherwise, even if the effect is still local to z_{n+1} with respect to η_n , *more* than the claimed number of images may be created; see [13, sect. 4.2] or [8, fig. 5]. This effect is also shown in the example in section 3. A quantification of this effect is subject of further research; see also [13].
7. The proofs in [13] show that in each of the cases the created images are located nearby (possibly rotated) roots of unity with radius *approximately* $\sqrt{m_{n+1}}$. The smaller the added mass m_{n+1} is, the closer the images assume these positions. The radii of the new images can be quantified; see [13, thm. 3.1].

Numerical examples for the cases 1–3 are shown in Fig. 1. The initial lens (top left image) is a binary lens with masses $m_1 = 0.6$ and $m_2 = 0.4$, external shear $\gamma = 0.5$, and a light source at $\zeta = 0$. The other three pictures (top right, bottom left, bottom right) display the effect of adding a small mass of $m_3 = 0.02$ at a position z_3 for each of the cases 1–3. As implied by Theorem 2.1, one, two and four images are created nearby the mass position z_3 , while the other images only alter their positions slightly. Examples for the case 4 with exactly one vanishing derivative of R are given in Section 3.

3 Construction of maximal point lenses

In the introduction we noted that the only known examples for maximal point lens models seem to arise from modifications of the point lens of Mao, Petters and Witt [9]. In this section we show how to construct from a

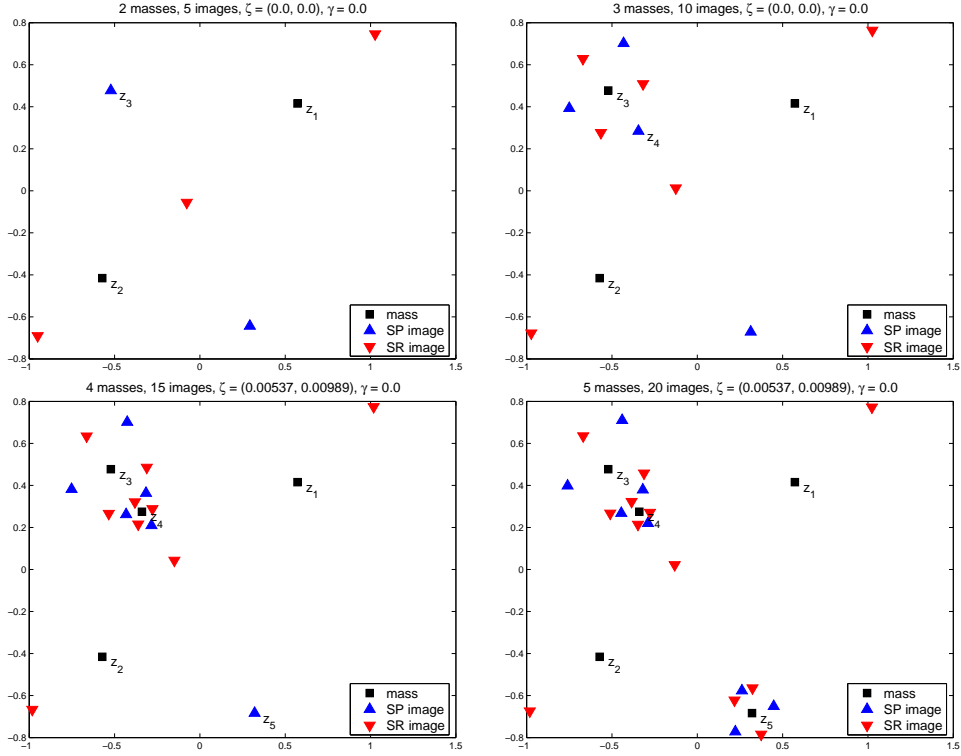


Figure 2: Numerical example for the image-creating effect of adding small masses at certain images of a maximal lens. See Section 3 for a detailed discussion. The symbols used are the same as in Fig. 1.

given maximal point lens on n masses another maximal point lens on $n + 1$ masses by adding a tiny mass to the given lens. The conditions we give are in fact a special case of Theorem 2.1, but applying this theorem to this *maximal lensing* case simplifies the conditions imposed on the lensing map η_n considerably and deserves a statement on its own. In the statement of this theorem we set the external shear γ to zero, but an analogous statement holds for gravitational lenses with external shear.

Theorem 3.1. *Let $\eta_n(z) = z - \sum_{j=1}^n \frac{m_j}{\bar{z} - \bar{z}_j} = z - \overline{R(z)}$ model a point lens on n masses $m_j > 0$ at positions $z_j \in \mathbb{C}$, that produces the maximal number of $5n - 5$ images. Let $z_{n+1} \in \mathbb{C}$ be an image with $R'(z_{n+1}) = 0$. Then for all sufficiently small masses $m_{n+1} > 0$, the lens modeled by the lensing map $\eta_{n+1}(z) = \eta_n(z) - \frac{m_{n+1}}{\bar{z} - \bar{z}_{n+1}}$, which is of degree $n + 1$, produces the maximal number of $5n$ images, provided that the source ζ does not lie on a caustic of η_n or η_{n+1} .*

Note that $R''(z_{n+1}) \neq 0$, because η_n is a maximal lens. Also, the image

z_{n+1} is necessarily an unmagnified image, since the magnification of z_{n+1} is

$$\text{Mag}(z_{n+1}, \zeta) = |\det D\eta(z_{n+1})|^{-1} = |1 - |R'(z_{n+1})|^2|^{-1} = 1.$$

The theorem is illustrated in Figure 2. The initial lens is depicted in the top left image. This binary lens with masses $m_1 = 0.6$ and $m_2 = 0.4$ at positions z_1 and z_2 and zero external shear produces five images of the source, thus it is a maximal lens. The projected position of the light source ζ on the lens plane is the origin. At the image z_3 indicated in the plot, we have $|R'(z_3)| \approx 5 \cdot 10^{-16}$, so the image z_3 satisfies (numerically) the condition of Theorem 3.1.

The result of adding a third mass of $m_3 = 0.05$ at z_3 is shown in the top right picture. As implied by the theorem, six “new” images around the newly created mass appear. As the “old” images only alter their positions slightly, but no image disappears (except for z_3), the constructed lens is maximal again.

After adding the mass m_3 at the position z_3 to the lens plane, the derivative of R does not vanish at any of the ten images. However, for the image z_4 indicated in the plot, we have $|R'(z_4)| \approx 0.0954$, which is already quite small. By shifting the projected source position ζ slightly within the caustic from $(0, 0)$ to approximately $(0.00537, 0.00989)$, the image z_4 moves to a nearby point in the lens plane, at which R' vanishes. Adding a mass of size $m_4 = 0.005$ at this displaced image again produces 6 new images in the vicinity of the newly added mass, and thus we have constructed a maximal point lens on four masses. The resulting lens configuration is shown in the bottom left plot.

Finally we wish to emphasize that the condition specified in Theorem 3.1, viz., that the derivative must vanish at the point where the mass is to be added, is only *sufficient* for obtaining again a maximal lens, but not necessary. It may well be that the maximum number of images, six, is already produced if the derivative is sufficiently small. This aspect is exemplified by the image z_5 in the bottom left plot. Here we have $|R'(z_5)| \approx 0.09$, but yet adding a small mass of $m_5 = 0.015$ produces six new images. Fewer images (four) are created, however, if m_5 is somewhat smaller, as implied by case 3 of Theorem 2.1. The resulting maximal lens is shown in the bottom right picture.

4 Conclusions and outlook

In this note we have presented a complete characterization of the image creating effect when a mass is inserted into a given microlensing model. The assumptions in the mathematical assertions cover microlensing models with and without shear and are applicable to any number of point masses. Our findings generalize a particular construction for maximal point lenses by Rhie

and we have given a general methodology for the construction of maximal point lens models.

The two most important open questions in the context of Theorem 2.1 are, firstly, to prove that the lower bounds on the number of created images are in fact equalities and, secondly, to quantify the allowable mass such that the claimed number of images are created.

Finally we mention that the question of maximal lensing in models with objects of radial mass density is much less understood than in point lens models [4].

Acknowledgements Robert Luce’s work is supported by Deutsche Forschungsgemeinschaft, Cluster of Excellence “UniCat”.

References

- [1] Jin H. An and N. Wyn Evans. The Chang-Refsdal lens revisited. *Monthly Notices of the Royal Astronomical Society*, 369(1):317–334, 2006.
- [2] Johann Bayer and Charles C. Dyer. Maximal lensing: mass constraints on point lens configurations. *Gen. Relativity Gravitation*, 39(9):1413–1418, 2007.
- [3] Johann Bayer and Charles C. Dyer. Erratum: Maximal lensing: mass constraints on point lens configurations. *Gen. Relativity Gravitation*, 41(3):669, 2009.
- [4] Dmitry Khavinson and Erik Lundberg. Gravitational lensing by a collection of objects with radial densities. *Anal. Math. Phys.*, 1(2-3):139–145, 2011.
- [5] Dmitry Khavinson and Genevra Neumann. On the number of zeros of certain rational harmonic functions. *Proc. Amer. Math. Soc.*, 134(4):1077–1085 (electronic), 2006.
- [6] Dmitry Khavinson and Genevra Neumann. From the fundamental theorem of algebra to astrophysics: a “harmonious” path. *Notices Amer. Math. Soc.*, 55(6):666–675, 2008.
- [7] Robert Luce, Olivier Sète, and Jörg Liesen. A Note on the Maximum Number of Zeros of $r(z) - \bar{z}$. *ArXiv e-prints*, October 2014. To appear in *Comput. Methods Funct. Theory*.
- [8] Robert Luce, Olivier Sète, and Jörg Liesen. Sharp parameter bounds for certain maximal point lenses. *Gen. Relativity Gravitation*, 46(5):1–16, 2014.

- [9] S. Mao, A. O. Petters, and H. J. Witt. Properties of point mass lenses on a regular polygon and the problem of maximum number of images. In *The Eighth Marcel Grossmann Meeting, Part A, B (Jerusalem, 1997)*, pages 1494–1496. World Sci. Publ., River Edge, NJ, 1999.
- [10] A. O. Petters and M. C. Werner. Mathematics of gravitational lensing: multiple imaging and magnification. *Gen. Relativity Gravitation*, 42(9):2011–2046, 2010.
- [11] Arlie O. Petters, Harold Levine, and Joachim Wambsganss. *Singularity theory and gravitational lensing*, volume 21 of *Progress in Mathematical Physics*. Birkhäuser Boston, Inc., Boston, MA, 2001. With a foreword by David Spergel.
- [12] S. H. Rhie. n-point Gravitational Lenses with $5(n-1)$ Images. *ArXiv Astrophysics e-prints*, May 2003.
- [13] Olivier Sète, Robert Luce, and Jörg Liesen. Perturbing rational harmonic functions by poles. *Comput. Methods Funct. Theory*, 15(1):9–35, 2015.
- [14] Norbert Straumann. Complex formulation of lensing theory and applications. *Helv. Phys. Acta*, 70(6):894–908, 1997.
- [15] Joachim Wambsganss. Gravitational lensing in astronomy. *Living Reviews in Relativity*, 1(12 (cited on May 12, 2014)), 1998.